AMERICAN SOCIETY FOR MICROBIOLOGY | Journal of Bacteriology

Trk2 Potassium Transport System in *Streptococcus mutans* and Its Role in Potassium Homeostasis, Biofilm Formation, and Stress Tolerance

Gursonika Binepal,[a] Kamal Gill,[a] Paula Crowley,[b] Martha Cordova,[a] L. Jeannine Brady,[b] Dilani B. Senadheera,[a] Dennis G. Cvitkovitch[a]

Department of Microbiology, Faculty of Dentistry, University of Toronto, Toronto, Ontario, Canada[a]; Department of Oral Biology, University of Florida, Gainesville, Florida, USA[b]

ABSTRACT

Potassium (K^+) is the most abundant cation in the fluids of dental biofilm. The biochemical and biophysical functions of K^+ and a variety of K^+ transport systems have been studied for most pathogenic bacteria but not for oral pathogens. In this study, we establish the modes of K^+ acquisition in *Streptococcus mutans* and the importance of K^+ homeostasis for its virulence attributes. The *S. mutans* genome harbors four putative K^+ transport systems that included two Trk-like transporters (designated Trk1 and Trk2), one glutamate/K^+ cotransporter (GlnQHMP), and a channel-like K^+ transport system (Kch). Mutants lacking Trk2 had significantly impaired growth, acidogenicity, aciduricity, and biofilm formation. [K^+] less than 5 mM eliminated biofilm formation in *S. mutans*. The functionality of the Trk2 system was confirmed by complementing an *Escherichia coli* TK2420 mutant strain, which resulted in significant K^+ accumulation, improved growth, and survival under stress. Taken together, these results suggest that Trk2 is the main facet of the K^+-dependent cellular response of *S. mutans* to environment stresses.

IMPORTANCE

Biofilm formation and stress tolerance are important virulence properties of caries-causing *Streptococcus mutans*. To limit these properties of this bacterium, it is imperative to understand its survival mechanisms. Potassium is the most abundant cation in dental plaque, the natural environment of *S. mutans*. K^+ is known to function in stress tolerance, and bacteria have specialized mechanisms for its uptake. However, there are no reports to identify or characterize specific K^+ transporters in *S. mutans*. We identified the most important system for K^+ homeostasis and its role in the biofilm formation, stress tolerance, and growth. We also show the requirement of environmental K^+ for the activity of biofilm-forming enzymes, which explains why such high levels of K^+ would favor biofilm formation.

Bacteria utilize specialized endogenous mechanisms to survive and proliferate in transient environments. A common bacterial response to environmental perturbations, such as acid stress, osmotic tension, and nutrient deprivation, is to accumulate certain solutes, such as potassium (K^+). K^+, a naturally abundant cation, is present in all types of cells and is essential for both cell survival and physiology. K^+ accumulation under stress conditions enables organisms to contend with dehydration, membrane damage, regulation of the Na^+/H^+-dependent cell energetics, and pH homeostasis while simultaneously minimizing interference with the structures and functions of intracellular proteins (1–3).

In prokaryotes, four main K^+ transport systems have been identified, which include the proteins Trk (or Ktr), Kdp, Kup, and channel-like Kch (4), all of which have different K^+ affinities. Their variety and independent functioning have likely evolved as a cell survival strategy to ensure that adequate levels of K^+ are present at all times to contend with environmental changes (5). These systems are responsible for maintaining a typical range of intracellular K^+ concentration, i.e., from 200 to 600 mM (6, 7).

Streptococcus mutans is an opportunistic oral pathogen which is a causative agent of dental caries (8). This bacterium can metabolize dietary sugars to produce acid end products (acidogenicity) and produces sticky insoluble glucan polymers for the formation of dental plaque. Furthermore, *S. mutans* can rapidly mount a pH stress tolerance response that allows its survival at pHs as low as 3.2 (9). The low pH in the plaque environment is a general growth-limiting factor which is modulated and favored by certain inhabitant bacteria and is distinct from other oral environments. It is known that the concentration of K^+ (80 mM) in the fluid portion of dental plaque is markedly higher than that of other cations found there, such as sodium (20 mM) and calcium (7 mM) (10, 11). Despite these findings, it is not well understood how such high K^+ concentrations affect physiology and virulence of oral bacteria such as *S. mutans*. It has been suggested that in response to acid stress, *S. mutans* can modulate its metabolic pathways by accumulating K^+ inside the cell (9, 12). According to previous reports, K^+ can affect growth and glycolytic activity (13, 14), membrane potential, and maintenance of cytoplasmic pH homeostasis (15, 16).

Received 2 October 2015 **Accepted** 13 January 2016

Accepted manuscript posted online 25 January 2016

Citation Binepal G, Gill K, Crowley P, Cordova M, Brady LJ, Senadheera DB, Cvitkovitch DG. 2016. Trk2 potassium transport system in *Streptococcus mutans* and its role in potassium homeostasis, biofilm formation, and stress tolerance. J Bacteriol 198:1087–1100. doi:10.1128/JB.00813-15.

Editor: A. Becker

Address correspondence to Dennis G. Cvitkovitch, d.cvitkovitch@dentistry.utoronto.ca.

G.B. and K.G. contributed equally to this work.

Supplemental material for this article may be found at http://dx.doi.org/10.1128/JB.00813-15.

Copyright © 2016, American Society for Microbiology. All Rights Reserved.

The *S. mutans* UA159 genome has at least four putative K^+ transport systems, annotated as Trk1, Trk2, Kch, and GlnQHMP (see Table S1 in the supplemental material). To gain an understanding of potassium acquisition and its role in *S. mutans* pathophysiology, isogenic mutants were used to measure K^+ transport. The main emphasis was to first elucidate the roles of two Trk systems in the main virulence attributes of *S. mutans* namely: acidogenicity, aciduricity, and biofilm formation. The role of GlnQHMP in modulating growth and acid tolerance of *S. mutans* UA159 has been reported (17). In the current study, we utilized the *glnQHMP*-null mutant to extend our knowledge regarding its role in K^+-dependent phenotypes. Beyond these systems, we also tested Kch, which is annotated as a hypothetical protein but has some sequence similarities with K^+ channel proteins.

To address our limitations in characterizing the K^+ uptake by putative K^+ transport systems individually in *S. mutans*, we cloned and expressed each system separately in an *Escherichia coli* mutant strain, TK2420, which is deficient in its three major K^+ transport systems (*kdp*, *trk*, and *kup*) (see Table S2 in the supplemental material). In the current study, we report that the distinctive K^+ transport system for *S. mutans* Trk2 is required for physiological adaptation of *S. mutans* under K^+-limited stress conditions. We show that the Trk2 system is required for regulating membrane potential and sugar metabolism. Finally, the Trk2 system is critical to the ability of *S. mutans* to form biofilms under low-K^+ conditions by regulating levels of glucosyltransferases and glucan production.

MATERIALS AND METHODS

Bacterial strains and culture conditions. *S. mutans* strains were grown in Todd-Hewitt yeast extract broth (THYE; BD, Sparks, MD) or minimal defined potassium-deprived medium with 1% glucose (MMGK) or with 1% sucrose (MMSK) at 37°C with aeration. MMGK was prepared as previously reported (18); potassium salts were replaced by sodium salts, and final concentrations of 5 mM cystine and 5 mM glutamic acid were added immediately before use. For growth under osmotic stress induced by 0.4 M NaCl, *S. mutans* strains were grown in chemically defined MMGK with 5 mM, 25 mM, and 50 mM KCl with or without 0.4 M NaCl. The *E. coli* strains were grown in Luria broth (Luria-Bertani broth; BD, Sparks, MD) or potassium-limiting medium (KLM) supplemented with 10 g/liter KCl for high-K^+ medium (HKLM) or with 10 g/liter NaCl for low-K^+ medium (LKLM) as described previously (19). Strains and primers used are listed in Table S2 in the supplemental material. To construct various K^+ transport system-null mutants, previously described PCR-ligation mutagenesis (20) was used.

Growth and stress tolerance. To monitor sensitivity to extracellular K^+ and determine the concentration for optimal growth, UA159 wild-type cells were grown in MMGK supplemented with 0 to 150 mM filter-sterilized KCl. Based on the results for growth response to K^+ of wild-type UA159 cells, the range of K^+ concentrations was then narrowed to 5 to 50 mM to monitor growth of various K^+ transport-null mutants. Growth was monitored in the Bioscreen C automated growth monitor (Lab Systems) as previously described (21). Briefly, 16 h cultures were diluted 1/20 in fresh THYE and grown to an optical density at 600 nm (OD_{600}) of at least 0.400. Cells were washed and resuspended in minimal medium to give equivalent OD_{600}s of ~0.040 and then plated in quadruplicate wells in a microtiter plate. Covered plates were placed in the growth monitor and maintained at 37°C for at least 18 h. Medium turbidity was measured at an absorbance of 600 nm every 20 min following 20 s of shaking. Static planktonic growth was assessed by diluting overnight cultures 1/20 in fresh THYE and measuring medium turbidity and medium pH from samples of a stock growth culture at selected time points. Medium turbidity was measured by placing samples in a 96-well plate and reading the optical density at an absorbance of 595 nm on a Bio-Rad model 3550 microtiter plate reader. In parallel, medium pH was measured using a VWR SB20 SympHony pH meter. The method used for *E. coli* strains was similar, with the following modifications: cells were grown and subcultured in HKLM and to test K^+ sensitivity, cells were subjected to low-K^+ medium (LKLM). For osmotic stress assays, test strains were grown in MMGK supplemented with specific concentrations of KCl with or without 0.4 M NaCl, and growth was monitored using the above-described protocol.

Acid stress response. The acid tolerance response (ATR) was assessed according to our published protocol (22). Briefly, overnight cultures were diluted 1/20 and grown to an OD_{600} of 0.400 in tryptone yeast extract (TYE) with 0.5% (wt/vol) glucose at pH 7.5. Half of the cultures were immediately placed in pH 3.5 TYE with 0.5% (wt/vol) glucose (kill medium) for up to 2 h and are referred to as unadapted cells/cultures. To obtain adapted cells, the other half of cultures was placed in TYE medium with 0.5% (wt/vol) glucose at pH 5.5 for 2 h prior to being placed in the pH 3.5 medium. Cells were pelleted via centrifugation at 4,000 × *g* for 10 min at 22°C and resuspended in the desired medium prewarmed to 37°C. Cultures were sampled at the 0-, 1- and 2-hour time points in the pH 3.5 medium, serially diluted, and plated in triplicate on THYE agar to obtain colony counts. Survival percentage was calculated as follows: (average colony count at postzero time point for a particular treatment/average colony count at the zero time point for the same treatment) × 100.

Biofilm staining and scanning electron and confocal laser scanning microscopy. Biofilms were grown as described previously (21) with a few modifications. Overnight cultures were diluted 1/50 in minimal medium and plated in 24-well Falcon tissue culture plates. Following a 20-hour incubation, cultures were dried and stained overnight with a 0.1% crystal violet dye solution. After removal of excess stain by rinsing with distilled H_2O, stained biofilms were imaged using a Canon Power Shot SD 1200 IS digital camera. Experiments were performed in quadruplicate wells and repeated four times. In parallel, biofilms were grown as described above but on glass slides and processed for scanning electron microscopy (SEM) as previously described (23).

For confocal analysis, 1 μM Texas Red-labeled dextran conjugate (molecular mass, 70 kDa; absorbance/fluorescence emission maxima of 595/615 nm; Molecular Probes, Invitrogen Corp., Carlsbad, CA) was added to the biofilm medium. All the bacterial cells in the biofilms were labeled with Syto 9 green fluorescent nucleic acid stain (485/498 nm; Molecular Probes) using a standard protocol (24, 25). The imaging was done using a Zeiss LSM700 confocal microscope at the Advanced Optical Microscopy Facility, University of Toronto. The plan-apochromat 60×/1.4 numerical aperture (NA) oil immersion (26) objective was used to obtain images. Two independent biofilm experiments were performed using the Thermo Scientific Nunc Lab-Tek II chambered cover glass with 8 wells, and 4 image Z-stacks at 1.0-μm intervals (512 by 512 pixels for quantification or 1,024 by 1,024 pixels for visualization) were collected for each experiment. The images were analyzed with the Imaris 7.0.0 software (Bitplane, Saint Paul, MN) and quantified for the average surface thickness and average spot objects of the biofilms.

qPCR analysis of *gtfB* expression. Expression of the *gtfB* gene in wtUA159 and the SMΔtrk2 mutant was assessed using quantitative real-time PCR analysis. Briefly, planktonic cultures were grown to an OD_{600} of ~0.4 in THYE. RNA was purified from both strains using methods described elsewhere (27), and *gtfB* was quantitated following PCR amplification with the primers 5′ ACACTTTCGGGTGGCTTG 3′ and 5′ GCT TAGATGTCACTTCGGTTG 3′. Expression change was normalized with the expression of the housekeeping 16S rRNA gene using the primers 5′-CTTACCAGGTCTTGACATCCCG-3′ and 5′-ACCCAACATCTCAC GACACGAG-3′. Using the Pfaffle method (28), the change (*n*-fold) in the expression in the mutant strain was calculated relative to expression of the *gtfB* gene in UA159. The change was calculated for at least 4 biological replicates and 3 technical replicates.

Western analysis of glucosyltransferase from cell surface extracts. Wild-type (UA159) and SMtrkΔ2 strains were cultured for 16 h in THYE broth at 37°C and passaged 1:20 in warm THYE. Growth was continued until an OD_{600} of ~0.6 was reached; then, cells were centrifuged, washed once in MMSK, and resuspended (1:20 dilution) in 40-ml tubes containing warm MMSK with KCl added at a 5, 25, or 50 mM final concentration. Cultures were grown 24 h at 37°C; then, cells were pelleted and washed twice in 20 mM Tris-Cl (pH 8.0) and extracted for 1 h with 1.0 ml of 4% SDS followed by boiling for 10 min, which allowed the extraction of noncovalently attached proteins from the cell surface without lysing the cells. Samples were centrifuged at 16,000 × *g*, and the supernatant was set aside for Western analysis. The OD_{280} of each SDS extract was measured using a Nanodrop 1000 spectrophotometer (ThermoScientific, Wilmington, DE), and extracts were standardized for protein concentration. Twenty micrograms of extract protein from duplicate cell cultures was applied to a 4-to-20% TGX gradient gel (Bio-Rad), and proteins were separated at 150 V. Separated proteins were blotted onto polyvinylidene difluoride (PVDF) membranes using the Transblot Turbo (Bio-Rad), and membranes were blocked overnight in PBS–0.3% Tween 20, 5% skim milk. Rat anti-GtfD antibody (29) was added to the blot at a 1:500 dilution, incubated for 1 h at room temperature, washed three times in PBS-Tween, and incubated for 1 h with 1:1,000 horseradish peroxidase (HRP)-conjugated goat anti-rat IgG. The blots were washed in PBS-Tween and developed using ECL-Prime (GE Lifesciences, Piscataway, NJ) for 1 min prior to imaging in the Gbox-Chemi XL1.4 imager (Syngene, Frederick, MD).

Visualization of glucan production from agar plate-grown colonies. *S. mutans* UA159 and the *trk2*-null mutant colonies were grown for 48 h on TSY20B (4% Trypticase soy agar, 0.5% plain agar, 1% yeast extract, 20% sucrose, and 0.2 U/ml of bacitracin; Thermo Fisher) plates at 37°C with an additional 72 h of incubation at 25°C. Colonies and glucan puddles produced were imaged with a Leica MZ8 dissecting microscope with a DFC320 camera and Firecam v.3.4.1 software (Leica Microsystems, Buffalo Grove, IL) using incident lighting. Magnifications were ×63 (smallest images) to ×160 (largest images).

Measurement of intracellular K^+ ion content. Overnight *S. mutans* cultures, diluted 1/20 in fresh THYE, were grown to an OD_{600} of 0.400. Cells were washed and incubated in MMGK without KCl for at least 2 h to deplete the cellular K^+. Cells were stimulated with 10 mM KCl, and an aliquot was taken and filtered (0.22 μm) every 30 s. The dry weights of filters for each sample were measured, and the filters were immersed in 10% HNO_3 and boiled for 30 min. Inductively coupled plasma optical emission spectroscopy (ICP-OES) was performed on each sample using an Optima 7300 DV instrument (PerkinElmer) housed at the ANALEST facility, Department of Chemistry, University of Toronto. Triplicate emission reads of samples were averaged and calibrated against a standard curve (minimum correlation of 99.9%) generated for different concentrations of potassium (766.49 nm) using a serially diluted QC4 standard (SCP Science, Quebec, Canada). For *E. coli* cultures, the overnight cultures grown were subcultured 1/20 in HKLM until they reached an OD_{600} of 0.4. Cells were then processed similarly to *S. mutans* cultures, as described above.

Membrane potential measurement using fluorescence. The alterations in electrical membrane potential of various wild-type and K^+ transport mutant cells were measured using the membrane-potential-sensitive fluorescent dye bis-oxonol {$DiSBaC_2(3)$ [bis-(1,3-diethylthiobarbituric acid) trimethine oxonol)]}. As bis-oxonol is an anionic, lipophilic molecule, a higher concentration of dye accumulates in the cell upon membrane depolarization, binding to intracellular components and resulting in an increase in cytosolic bis-oxonol fluorescence intensity, whereas upon hyperpolarization, less dye is located intercellularly and fluorescence intensity decreases.

Overnight *S. mutans* cultures, diluted 1:20 in fresh THYE, were grown to an OD_{600} of 0.4. Cells were then washed and resuspended in MMGK supplemented with defined KCl, with or without stressors such as pH or osmotic stress. A 100-μl portion of cell suspension was aliquoted in a 96-well plate and mixed with fluorescent dye reaction mixtures prepared using the FIVEphoton kit manufacturer's protocol (FIVEphoton Biochemicals). The plate was incubated for 15 min and fluorescence emission intensity (emission wavelength of 560 nm) was measured using a TECAN microplate reader (excitation wavelength of 530 nm). The plate conditions were set at 37°C with shaking for 5 s before every read, and the fluorescence emission intensity measurement was taken every 15 min for at least 6 h. For *E. coli* strains, the experimental protocol followed was the same as for *S. mutans* with the following modifications: cultures were grown in HKLM and the mid-exponential-phase cells were washed and resuspended in either MMGK with defined concentrations of KCl, or cells were resuspended in KLM medium with low and high K^+ content and test stressors. The measurement protocol was altered to accommodate desired culture conditions at 37°C with continuous shaking and read every 2 min for at least 6 h. For fluorescence intensity change analysis, data were transformed to control for bias potentially generated by experimental setting variations: fluorescence was expressed as change between time *t* and time zero according to the following formula: $\Delta F_t = [(F_t - F_0)/F_0]$ (30). To control for intensity change of the dye, ΔF_t (culture sample) was normalized with ΔF_t (blank with dye), and final values were plotted against time for each condition used.

Complementation assay. The *E. coli* strain TK2420 (4) was a generous gift from Wolfgang Epstein (University of Chicago). Open reading frames (ORFs) for each K^+ transport system (*trk-1*, SMU_1561-63; *trk-2*, SMU_1708-09; *glnQHMP*, SMU_1519-22; and putative *kch*, SMU_1848) were each amplified using specific primers and cloned into the pET-DUET expression vector (Novagen, Inc.). DNA sequencing confirmed proper ligation of inserts into expression vectors. Complementation was assayed as described previously (31), with a few modifications. Briefly, competent TK2420 cells were heat shock transformed with each expression vector of interest and grown with ampicillin selection on potassium-rich (HKLM) agar. Colonies were then restreaked on low-potassium (LKLM) agar with ampicillin selection to confirm successful complementation. Starter cultures were grown overnight by inoculating single colonies in HKLM with ampicillin. Subsequently, cultures were grown to mid-exponential phase, washed and resuspended in sterile H_2O or PBS, and serially diluted before being plated as 10-μl droplets on MMGK agar.

RESULTS

K^+ transport systems identified in *S. mutans*. The *S. mutans* UA159 genome harbors two orthologs of putative K^+ transporters, which are designated Trk1 and Trk2 (Fig. 1; also, see Table S1 in the supplemental material). A Conserved Domains Database (CDD) search was used to elaborate the predicted protein domains and families (32). The predicted interactive partners and proteins that share sequence identity in other bacteria are listed in Table S1 in the supplemental material. The Trk1 system is annotated to be comprised of TrkB, Trk, and PacL and is encoded by a tricistronic operon. Both TrkB and Trk are predicted to contain N-terminally conserved Rossmann fold NAD^+-binding regions with a GXGXXG consensus sequence. This motif is known to confer specificity to NAD^+ binding through its first two glycine residues. Glycine-rich regions are also found and associated with selectivity for K^+ ions. The C-terminal ends of these proteins have a predicted conserved permease-like domain, which is conducive to configuring its beta structure and has specificity for an unknown ligand. PacL has four predicted conserved domains that include an N-terminal cation ATPase, an E1-E2 ATPase (Pfam 00122), a conserved putative hydrolase of Na^+/K^+ ATPase alpha-subunit like domain, and a C-terminal cation ATPase.

The Trk2 putative K^+ transport system in *S. mutans* is comprised of two components, TrkA and TrkH, whose encoding genes form a bicistronic operon. The TrkA is predicted to have con-

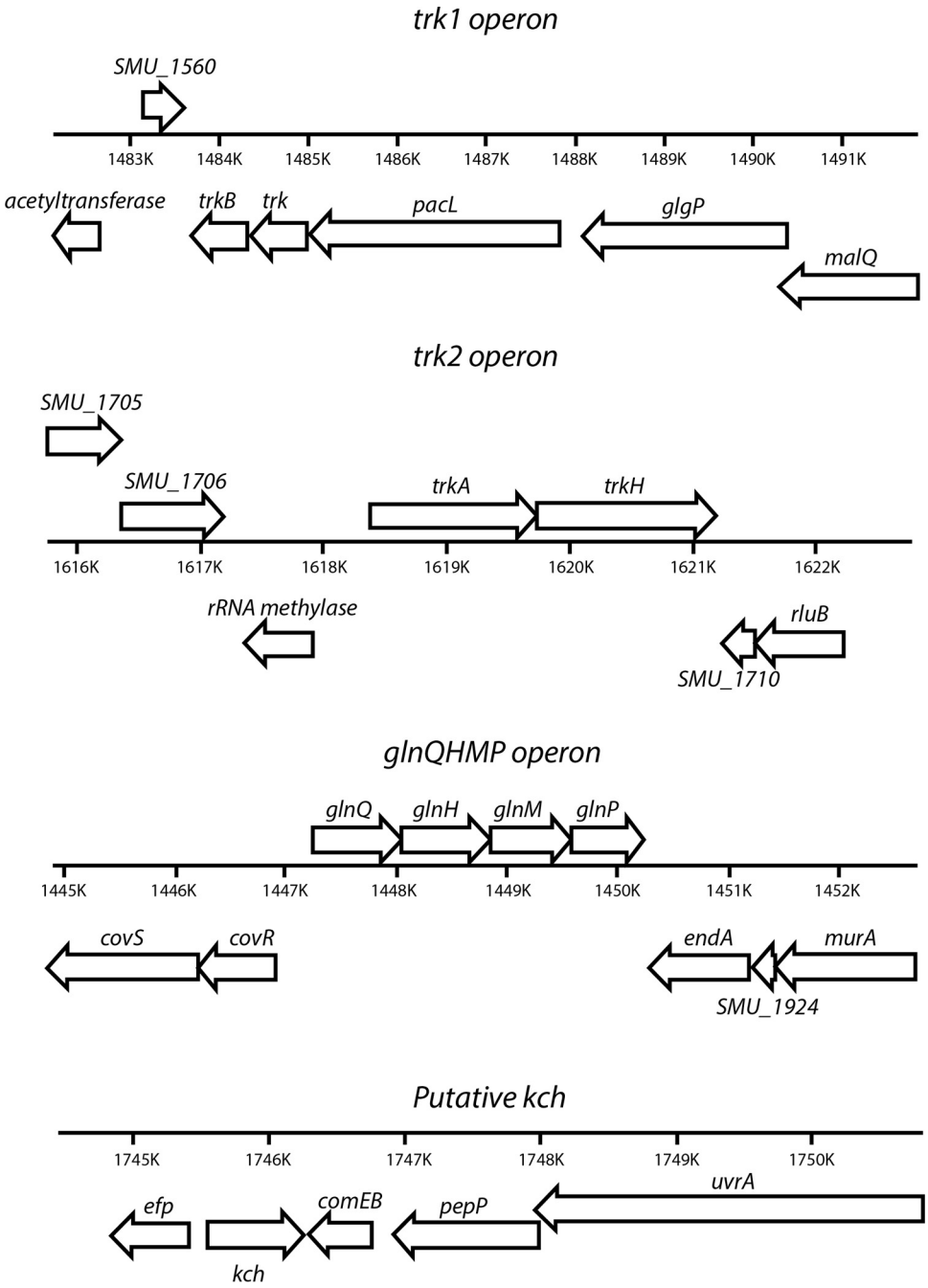

FIG 1 Genetic map of operons encoding the putative K^+ transport systems in *Streptococcus mutans* UA159.

served domains similar to those observed for TrkB (of the Trk1 system) with a Rossmann fold NAD^+-binding region. TrkH is believed to form a complex with TrkA and is a transmembrane component.

In addition to Trk1 and Trk2, other putative systems that could modulate the transport of K^+ in *S. mutans* are the GlnQHMP (17), and Kch. Kch is a hypothetical protein in the *S. mutans* UA159 chromosome encoded by *SMU_1848* (NCBI) with high homology to conserved ion channel-like domains of either two helices or a tetrameric structure and belongs to the family of pfam07885, which has a conserved GYG sequence shown to result in glycine-rich selectivity for K^+ ions (33).

Role of K^+ in *S. mutans*. To understand the roles of Trk1, Trk2, GlnQHMP, and Kch in *S. mutans* physiology, isogenic mutant strains deficient in individual operons (strains SMΔtrk1, SMΔtrk2, SMΔglnQHMP, and SMΔkch) and knockout mutants deficient in genetic components of these systems (strains SMΔtrk, SMΔtrkB, SMΔtrkA, SMΔtrkH, and SMΔpacL) were used (see Table S2 in the supplemental material). To examine the effects of both Trk systems, we constructed a double-knockout mutant

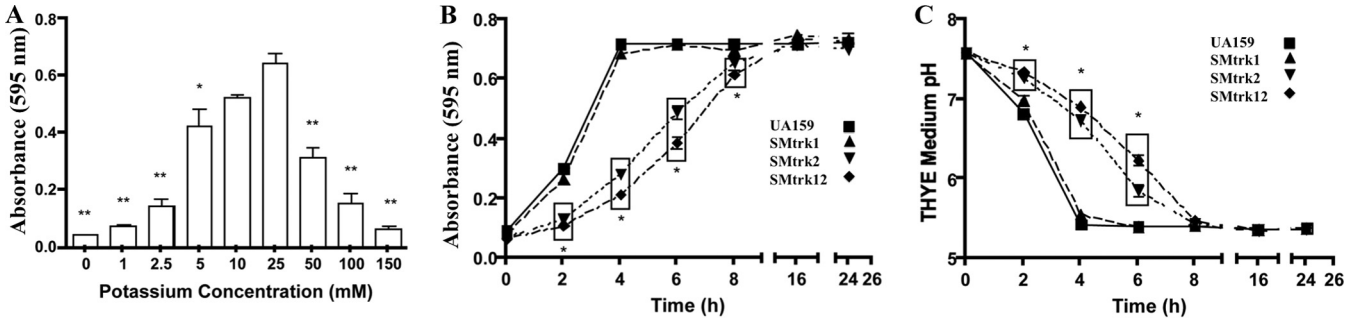

FIG 2 Effects of K^+ and its transport systems in growth and final pH changes in *S. mutans*. (A) Growth analysis of the parent strain *S. mutans* UA159. Final absorbance measurements were taken from cell cultures grown in MMGK supplemented with various concentrations of KCl (0 mM to 150 mM). (B) Growth curves of wild-type and Trk mutants grown in K^+-rich THYE medium (~19 mM). (C) pH measurements of the Trk1, Trk2, and Trk1/Trk2 mutants grown in THYE growth medium over time. Asterisks indicate that the values are statistically significantly different from that for growth in 25 mM K^+ (A) or from that for the WT (B and C) (*, $P < 0.05$; **, $P < 0.001$). Values are means and standard errors (SE) from experiments repeated three times, and statistical comparison was performed using a two-way analysis of variance (ANOVA).

strain lacking *trk1* and *trk2* operons, designated SMΔtrk12 (see Table S2 in the supplemental material).

(i) K^+-dependent-growth characterization. The concentrations of K^+ required for optimal growth of *S. mutans* and the K^+ concentrations present in some commonly used growth media (THYE, TYE, and MMGK; described in Materials and Methods) were measured using inductively coupled plasma optical emission spectroscopy (ICP-OES). Our results indicated that both THYE and TYE had sufficient but not optimal concentrations of K^+ (>10 mM) for the growth of *S. mutans* (see Table S3 in the supplemental material). To test the effect of limited K^+, the planktonic growth of *S. mutans* UA159 wild-type strain was tested in MMGK medium supplemented with a range of K^+ concentrations (5 to 150 mM), and growth was monitored using the Bioscreen C automated growth monitor. By comparing the final absorbance values (Fig. 2A) for growth, we noted that optimal growth was accomplished in MMGK supplemented with 25 mM K^+. At this concentration, the growth yield was significantly higher than that at ≤5 mM or ≥50 mM K^+ ($P < 0.01$). For our experiments (unless otherwise stated), we used MMGK medium supplemented with (i) 5 mM K^+ (low-K^+ conditions), (ii) 25 mM K^+ (optimal conditions), and (iii) 50 mM K^+ (high-K^+ conditions).

(ii) Role of K^+ transport systems in growth. The roles of the Trk1- and Trk2-dependent K^+ acquisition on the growth of *S. mutans* were examined in K^+-rich THYE medium. Notably, loss of the *trk2* operon (SMΔtrk2) and the combined *trk1 trk2* deletion mutant (SMΔtrk12) resulted in significantly reduced growth yields at the 2-, 4-, 6- and 8-hour time points relative to the wild type and the *trk1* knockout mutant ($P < 0.01$) (Fig. 2B). Concomitant with the growth defect, we noted that the drop in pH values was slower than in the parent strain, reflective of significantly reduced acid production by strains SMΔtrk2 and SMΔtrk12 ($P < 0.001$) (Fig. 2C). Further, the growth retardation of the *trk2*-deficient strain was observed to be consistent when cells were grown under low-K^+ conditions in the presence of various dietary sugars, such as fructose, sucrose, mannose, and glucose (data not shown). Unlike the Trk systems, loss of the Kch system did not have a considerable effect on the growth phenotype of *S. mutans* (data not shown).

(iii) Trk2 is essential for acid stress tolerance. The acid tolerance response of *S. mutans* is a major virulence attribute that fa-

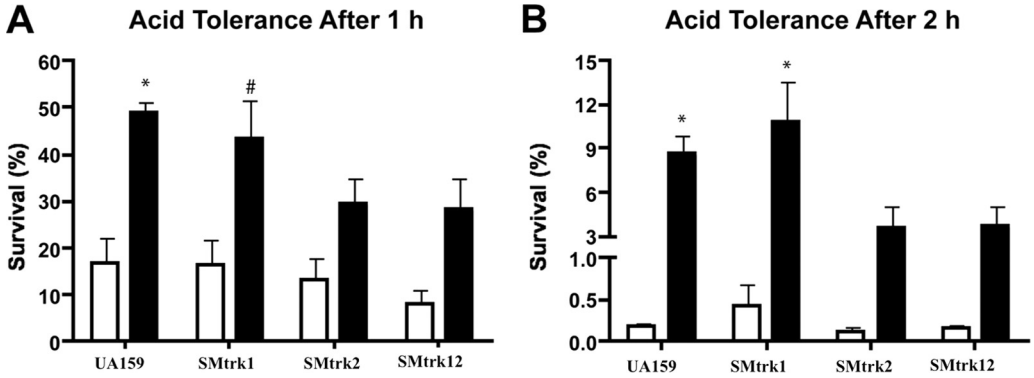

FIG 3 Acid stress response of *S. mutans* wild-type strain UA159 and Trk mutants. Acid tolerance assays were conducted with unadapted (white bars) and adapted (black bars) cultures incubated for 1 h (A) or 2 h (B) at a killing pH of 3.5. For pH adaptation, cells were preexposed to TYE medium plus 0.5% glucose that was adjusted to pH 5.5. After exposure to the killing pH, cells were plated, and acid tolerance was expressed as percent survivors relative to the total number of CFU present at time zero, just prior to exposure at pH 3.5. #, $P < 0.01$, and *, $P < 0.001$, compared to unadapted cultures of the same strain. Values are means and standard errors (SE) from experiments repeated three times, and statistical comparison was performed using a one-way ANOVA.

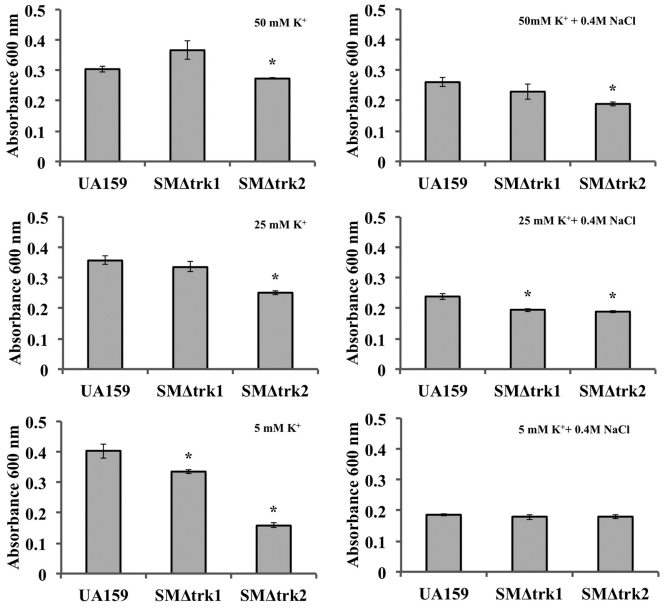

FIG 4 Osmotic stress adaptation of wild-type UA159 and SMΔtrk2 in limited K^+. Strains were grown in MMGK with 5 mM, 25 mM, and 50 mM KCl for 24 h. To examine growth rate under osmotic stress, cells were supplemented with 0.4 M NaCl (right) and compared to those without NaCl (left). Final growth yields in various K^+ concentrations with or without 0.4 M NaCl for four biological and three technical replicates are presented. Student's *t* test was used to determine statistical significance (*, $P < 0.05$) compared to wild-type strain UA159.

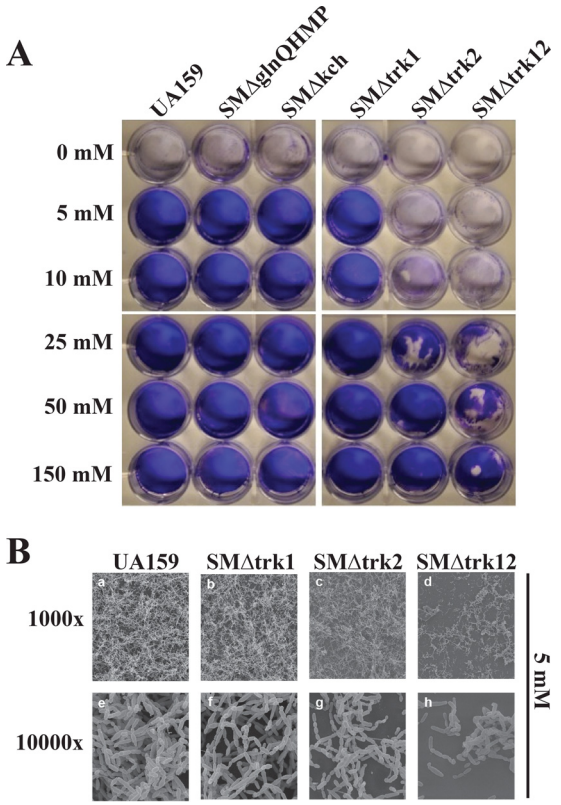

FIG 5 Evaluation of biofilm production with scanning electron microscopy for *S. mutans* wild-type strain UA159 and mutant strains deficient in primary K^+ transport systems. (A) Biofilms were grown on microtiter plates in MMGK supplemented with various concentrations of KCl (0 to 150 mM). After a 20-hour incubation, supernatant was removed and biofilms were dried and stained with 0.1% crystal violet dye. The experiment was repeated at least three times using triplicate wells each time. Representative photographs are shown. (B) Biofilms were grown on glass coverslips placed in microtiter plates containing MMGK supplemented with 5 mM. Following a 20-hour incubation period, biofilms were dehydrated and further processed for SEM. Representative micrographs are shown.

cilitates its survival under low-pH conditions (pH < 3.5) that are often detrimental to other competing oral bacteria. When supplemented with sugars, *S. mutans* produces acid end products, primarily lactic acid, which decreases its environmental pH. When preexposed to a mildly acidic signal (pH 5.5), *S. mutans* can activate protective mechanisms for survival at a killing pH (pH 3.5) (34, 35). To examine the role of Trk1 and Trk2 systems in the ATR of *S. mutans*, we quantified survival using acid killing assays with acid-adapted or unadapted cultures. In agreement with other studies, adaptation to acid significantly increased the survival rates of the *S. mutans* wild-type strain UA159 (Fig. 3). Although this was the case with the Trk1 deletion mutant, loss of Trk2 did not show a significant difference in percentage viability between adapted and unadapted cells (Fig. 3). As observed with the growth phenotypes, the response to acid killing of the Trk2 mutant was similar to that of the Trk1/Trk2 double mutant, suggesting the importance of Trk2 for the acid stress response of *S. mutans*. In contrast to the Trk1/Trk2 systems, tolerance of *S. mutans* to acid stress was not affected by the deletion of the Kch system (data not shown).

(iv) Role of K^+ in osmoregulation. K^+ accumulation is an essential aspect of bacterial response to osmotic stress. Perturbations in environmental osmolality of oral biofilms can significantly affect the overall cell energetics and expression of various systems involved in survival and virulence of *S. mutans* (36). To assess the influence of the putative K^+ transport systems on osmoadaptation, we tested the growth of mutant and wild-type *S. mutans* strains under osmotic stress induced by 0.4 M NaCl in MMGK medium supplemented with low (5 mM), optimal (25 mM), and high (50 mM) concentrations of K^+. The cultures were depleted of K^+ prior to growth analysis by first incubating cells in MMGK for 1 h. At a low concentration of K^+ (5 mM), the growth of SMΔtrk2 was significantly reduced compared with that of UA159 (Fig. 4). However, increasing the concentration of K^+ to 25 mM or 50 mM improved the growth of *trk2* mutant strains relative to that seen under low-K^+ conditions. In a low K^+ concentration and with an osmotic stress of 0.4 M NaCl, growth retardation was observed for all test strains. Although the growth alterations in response to various concentrations of K^+ were weak, we did observe that a K^+ concentration of 25 mM in MMGK improved the growth of UA159, and a higher concentration of 50 mM improved that of SMΔtrk1 under osmotic stress, while the growth of SMΔtrk2 remained low even in the presence of 50 mM K^+. Thus, we concluded that Trk2 is most important for K^+-mediated osmoadaptation in *S. mutans*.

Biofilm formation in limited K^+ requires the Trk2 system. The ability of *S. mutans* to form a biofilm is critical to its survival in the oral cavity (37, 38). So far, the biofilm phenotype of *S. mutans* and its relationship with K^+ transport systems have not been examined. We examined the biofilm formation of the K^+ transport mutant strains in MMGK supplemented with defined

concentrations of K^+ (0 to 150 mM). Without K^+ in the growth medium (0 mM), biofilm formation was completely abolished for wild-type UA159 and mutant strains (Fig. 5A). When supplemented with 5 mM K^+, the SMΔtrk2 strain formed a fragile and extremely thin biofilm compared to the parent strain. Biofilms formed by the Trk1/Trk2 double mutant were also unstable and easily disrupted relative to those of the wild type and the Trk2 mutant. We observed a restoration of the biofilm phenotype of SMΔtrk12 at a K^+ concentration of 150 mM. Although the discrepancy in the biofilm phenotype between SMΔtrk2 and SMΔtrk12 mutants suggested an influence of Trk1 on biofilm formation, we did not notice an impairment of the biofilm phenotype with the loss of Trk1 alone. In contrast to the influence of Trk systems in biofilm formation, loss of the GlnQHMP and Kch systems did not affect the biofilm phenotype relative to that of the wild type under test conditions.

Scanning electron microscopy for wild-type or Trk1 knockout strains grown in 5 mM K^+ (Fig. 5B) showed normal entangled chains of spherical cells. In contrast, SMΔtrk2 and SMΔtrk12 mutant biofilms contained fewer cells forming less entangled and shorter chains than the parent strain. These defects were more pronounced in the double knockout, as revealed by crystal violet staining (Fig. 5A). Supplementation with excess K^+ (>50 mM) recovered the biofilm phenotypes in the mutant strains. Since we had previously noted that loss of Trk2 affected growth of *S. mutans*, we tested whether the Trk2-mediated biofilm phenotype was related to a growth deficiency or the result of compromised cell viability. Our live/dead stains of the Trk biofilms with PI and Syto 9 showed that cell viability was not affected in the SMΔtrk2 mutant strain relative to the wild type (K. Gill, unpublished data).

qRT-PCR analysis was done for the expression of *gtfB* in SMΔtrk2 relative to wild-type (WT) UA159 in mid-logarithmic growth phase. The expression of *gtfB* relative to WT UA159 was 0.5 ± 0.12 in the planktonic cultures of SMΔtrk2, which was 2-fold downregulated. Although this was not statistically different from the expression in WT UA159, the downregulation led us to further investigate if biofilm formation was disrupted in the *trk2*-null mutant under low K^+ concentrations, since glucosyltransferase activity is affected in these mutants. To test this, we grew biofilms of SMΔtrk2 and UA159 strains in minimal medium with sucrose (MMSK) instead of glucose and tested glucan formation in low and high K^+ concentrations using confocal laser scanning microscopy analyses. With sucrose as the sugar source, the incorporation of Texas Red-labeled dextran into newly synthesized glucan was measured as a function of Gtf activity. The assembly of the extracellular matrix was measured by incorporating Texas Red-dextran at the beginning of the biofilm assay, with the cells also having been stained with Syto 9 to discriminate the glucan from cell material. The (fluorescently labeled) dextran acts as a primer and acceptor for GtfB and is incorporated with the help of Gtf proteins into the extracellular polymeric substance (EPS) matrix over the course of biofilm formation (24, 39). The amount of biofilm EPS produced by the SMΔtrk2 mutant (Fig. 6) was significantly lower than that produced by the wild-type strain UA159 at 25 and 50 mM K^+, while no difference between the two strains was observed at 5 mM K^+. A similar result was seen for cell scores (Fig. 6) at all K^+ concentrations. Significant increases in cell number and biofilm thickness were observed at 25 and 50 mM K^+ for the wild-type strain. To normalize the Gtf activity to total cell count, total dextran thickness was measured and normalized to the total number of Syto 9-stained cells, with the final dextran thickness per cell presented in Fig. 6. Compared with results observed under low-K^+ conditions, there was a significant increase in the EPS thickness per cell observed in the presence of 25 mM K^+ for the WT strain UA159, while EPS thickness per cell for SMΔtrk2 increased in the presence of 50 mM K^+. Although we were able to see some biofilm formation by the SMΔtrk2 mutant under low K^+ conditions using sucrose as the sugar source, that was not observed using the previous method (Fig. 5), but the SMΔtrk2 biofilm remained significantly impaired relative to that of UA159.

Western blot analysis was then carried out to further examine if low intracellular K^+ levels in the *trk2*-null mutant caused a defect in Gtf levels in the SMΔtrk2 mutant compared with UA159 under conditions of limited K^+ (Fig. 7A). Using polyclonal anti-GtfD sera, we observed a reduction in levels of SDS-extracted, cell-associated GtfD in the mutant at all medium-K^+ concentrations. Notably, the protein profiles for UA159 (WT) were different from those for the *trk2*-null mutant in the Gtf MW region (~155 kDa), with high molecular-mass bands being prominent for UA159 and lower-molecular mass bands (~30 kDa) that did not react with the antibody being prominent in the mutant. For further confirmation, the presence or absence of glucan puddles for both UA159 and SMΔtrk2 was monitored on sucrose-rich-medium plates. Interestingly, large clear glucan puddles could be seen around the UA159 colonies (Fig. 7B), where none could be seen around the SMΔtrk2 mutant colonies, although colonies of the latter glistened, suggesting the presence of modest amounts of glucan. Taken together with the Western analysis data, this suggested that glucosyltransferase activity, and hence glucan production, is severely impaired in the Trk2 mutant.

K^+ acquisition by *S. mutans*. Despite the critical role of K^+ in growth, glycolysis, and stress tolerance of *S. mutans*, there are no studies to date examining how this organism acquires K^+. To establish a clear role for Trk1, Trk2, GlnQHMP, and Kch in K^+ acquisition, we used ICP-OES for quantifying the K^+ transported by each null mutant relative to wild-type UA159 over time. First we measured the temporal intracellular concentrations of K^+ with respect to extracellular supplemented concentrations of KCl (5, 10, 25, and 50 mM) in the growth medium MMGK (data not shown). Prior to analysis, we ensured cell depletion of K^+ by incubation in MMGK for at least 2 h. For Trk1, GlnQHMP, and Kch deletion mutants, growth, as assessed by dry weight measurement of each cellular sample, was unaffected at 5 mM K^+, while at this concentration, the Trk2 mutants were unable to grow, leading us to conclude that K^+ uptake did not occur in Trk2 mutants (data not shown). When K^+ in the medium was increased to 50 mM, we did not observe statistically significant differences in growth or total K^+ uptake in any of the mutants relative to those of the wild type (see Fig. S4 in the supplemental material). To compare K^+ uptake in wild-type versus mutant cells, we used cells grown in MMGK supplemented with either 10 mM or 25 mM KCl, to determine initial and prolonged K^+ uptake, respectively. With media supplemented with 10 mM K^+, the intracellular content of K^+ increased significantly over time (15 s to 2 min) for SMΔtrk1 (up to 1.22 ± 0.5 μmol/mg [dry weight] of cells) relative to the wild type (0.28 ± 0.05 μmol/mg [dry weight] of cells). However, no significant differences in intracellular K^+ concentration were observed between UA159 and the mutant strains SMΔtrk12, SMΔkch, and SMΔglnQHMP (Fig. 8A).

Since we observed growth defects in SMΔtrk2 at 25 mM K^+

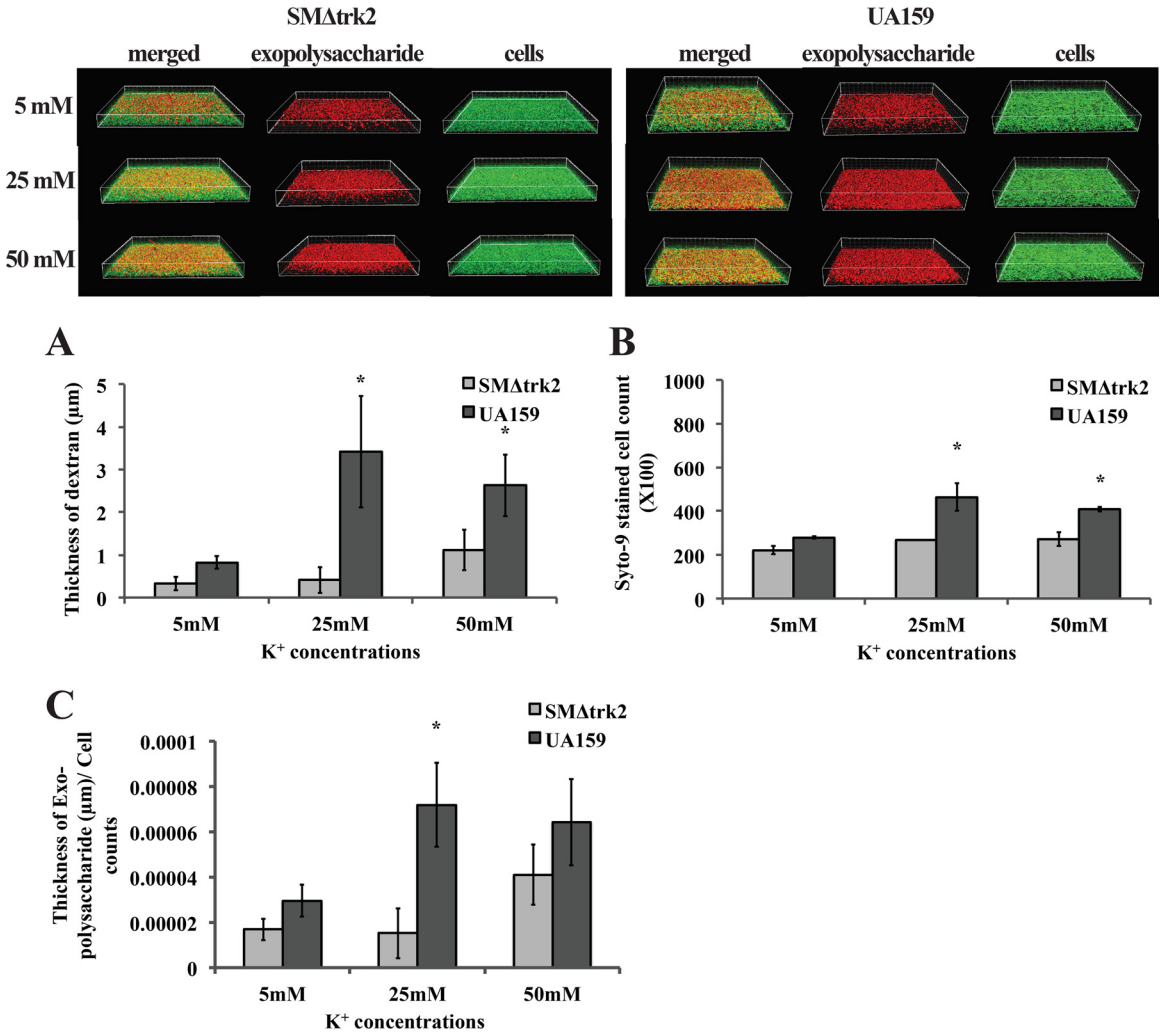

FIG 6 Confocal laser scanning microscopy of biofilms formed by *S. mutans* wild-type strain UA159 and *trk2*-null mutant strains. Biofilms were grown on an 8-well chambered cover glass containing MMSK supplemented with 5 mM, 25 mM, or 50 mM KCl and 1 μM Texas Red-labeled dextran conjugate. At 18 h, all of the bacterial cells in the biofilms were labeled with Syto 9 green fluorescent nucleic acid stain and processed for confocal laser scanning microscopy (CLSM). The histograms represent the average surface thickness of dextran (A), average spot counts of objects in the biofilms (B), and the dextran thickness normalized to the Syto 9-stained-cell count (C). Values are means and standard errors (SE) from experiments repeated three times with three technical replicates, and statistical comparison was performed using Student's *t* test. A *P* value of <0.05 was considered significant (*).

that were overcome by the medium being supplemented with 50 mM K^+, we used a K^+ concentration of 25 mM to test whether its growth retardation was due to the lack of adequate intracellular K^+. We also assessed K^+ accumulation in various isogenic Trk1 and Trk2 mutants relative to that of the wild type supplemented with 25 mM K^+ after an extended time of 30 min (Fig. 8B). At 30 min, K^+ accumulation by the strain deficient in both Trk1 and Trk2 was significantly reduced compared to that of UA159 cells ($P < 0.01$). Moreover, as previously observed with similarities in biofilm and acid tolerance phenotypes, the SMΔtrk12 had comparable levels of intracellular K^+ relative to the SMΔtrk2 mutant (0.118 ± 0.029 μmol/mg [dry weight] of cells and 0.115 ± 0.039 μmol/mg [dry weight] of cells, respectively). Our results showed that UA159 could accumulate high levels of K^+ (0.295 ± 0.025 μmol/mg [dry weight] of cells) compared with potassium-starved UA159 cells (0.060 ± 0.021 μmol/mg [dry weight] of cells) ($P < 0.001$). The amount of cellular K^+ was not statistically different between K^+-starved UA159 and mutant strains (0.113 ± 0.023 μmol/mg, 0.11 ± 0.011 μmol/mg, and 0.08 ± 0.009 μmol/mg [dry weight] of cells for SMΔtrk1, SMΔtrk2, and SMΔtrk12, respectively).

Influence of K^+ transport systems on the membrane potential of *S. mutans*. The transmembrane potential of bacterial cells is a critical feature governing growth and cell physiology by affecting cellular proton motive force, pH homeostasis, protein function, and protein localization (40). Here, we examined the role of K^+ transport systems in maintaining the membrane potential of *S. mutans* in response to changes in external K^+ concentrations. We had observed that the loss of Trk1 and Trk2 systems had a profound effect on growth, stress tolerance, and K^+ acquisition of *S. mutans*. After washing *S. mutans* strains with K^+-deficient growth medium, we challenged cells with 0, 5, 25, and 50 mM K^+ in MMGK with and without acid stress. Membrane potential assays were then conducted by measuring the fluorescence intensity of a

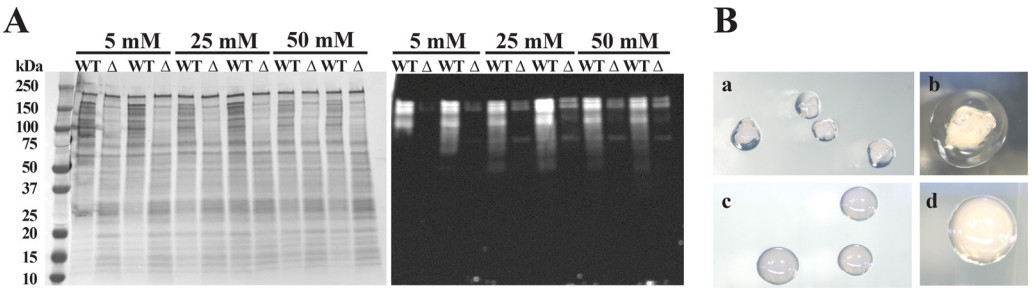

FIG 7 (A) Western blot analysis for glucosyltransferase derived from cell surface protein extracts of wild-type *S. mutans* and SMΔtrk2 grown in MMSK with various KCl concentrations. Twenty micrograms of SDS-extracted cell surface proteins from 24-h duplicate cultures of wild-type and *trk2*-null mutant strains grown in MMSK with 5, 25, and 50 mM KCl were separated on 4-to-20% TGX gradient gels, blotted, and stained for total protein (left) or probed with anti-GtfD (right). (B) Glucan production by *S. mutans* wild-type (a and b) and *trk2*-null mutant (c and d) strains. Strains were grown on TSY20B (20% sucrose) agar plates for 48 h at 37°C and an additional 72 h at 25°C. Colony morphology was imaged using a Leica MZ8 dissecting microscope with DFC320 camera and Firecam v.3.4.1 software (Leica Microsystems, Buffalo Grove, IL) using incident lighting. Magnification, ×63 (a and c) and ×160 (b and d).

potentiometric dye, $DiSBAC_2(3)$, that can enter only a depolarized cell or a cell with high cation accumulation (41). We analyzed the membrane potential of wild-type UA159, SMΔtrk1, and SMΔtrk2 mutants after 15 min, 30 min, and 2 h (see Fig. S1 in the supplemental material). The wild-type strain UA159 showed high depolarization at 5 mM K^+ at pH 5.5, which was in contrast to the mutants lacking *trk1* or *trk2* (see Fig. S1 in the supplemental material). While the *trk1* mutant showed recovery at 25 mM K^+ concentration, the *trk2* mutant showed recovery only at a 50 mM K^+ concentration at pH 5.5. The defect in K^+ gradient-dependent membrane potential of SMΔtrk2 mutants under pH 5.5 stress suggested a link between Trk2-mediated K^+ homeostasis and the defect observed in acidogenicity and aciduricity of this mutant.

Characterizing *S. mutans* K^+ transport systems in *E. coli* strain TK2420. Our aim was to dissect the function of each of the *S. mutans* K^+ transport systems individually, which we were unable to do using the parent strain under our test conditions. The genes containing the four *S. mutans* K^+ transport systems were cloned into the pET-DUET cloning and expression vector and transformed into *Escherichia coli* TK2420, which lacks its own constitutive K^+ transport systems. The complementation of these systems was confirmed by selection on high- and low-K^+ plates with ampicillin. We also included recombinant plasmids containing the individual components of the Trk systems to determine whether these proteins can function independently. We were able to obtain clones on low-K^+ agar plates for strains harboring plasmids that contained *pacL*, *glnQHMP*, *trk2*, or *kch. trk1a* of the Trk1 system containing peripheral *trkB* and *trk* components and TrkA or TrkH of the Trk2 system did not complement *E. coli* TK2420, as deduced by a lack of colonies on low-K^+–ampicillin plates.

***E. coli* TK2420 incorporated with *S. mutans* K^+ transport systems recovers K^+ acquisition and growth.** Previously, it was reported that in *E. coli* TK2420, K^+ uptake by nonspecific trans-

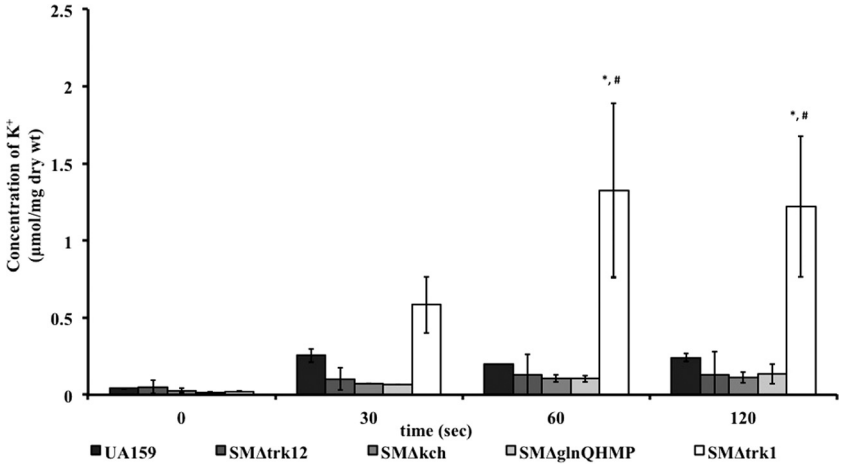

FIG 8 (A) Estimation of intracellular K^+ content in *S. mutans* wild-type UA159 strain and K^+ transport knockout mutants. To deplete cells of K^+ prior to uptake assays, mid-exponential-phase cells were incubated in K^+-deficient MMGK growth medium for 2 h. Cells were then supplemented with 10 mM KCl, and aliquots were sampled over time to measure intracellular K^+ content using ICP-OES. Values are means ± standard deviations for at least four biological and two technical replicates. Repeated-measures ANOVA was performed, and comparisons were made between different time points within each group (*) and by comparing intracellular K^+ levels between groups (#); a P value of <0.05 is considered significant. (B) Intracellular K^+ accumulation after 30 min. Wild-type UA159 and knockout mutant strains were grown to an OD_{600} of ~0.4 in THYE medium prior to incubation in minimal medium for 10 to 12 h to deplete cellular K^+. Cells were subsequently challenged with 25 mM K^+ for 30 min followed by measurement of cellular cation content via ICP-OES. Values are means and SE; experiments were repeated at least four times, and statistical comparison was performed using a two-way ANOVA. *, $P < 0.01$ compared to the value for WT cells stimulated with 25 mM K^+; #, $P < 0.01$ compared to the value for WT cells starved of K^+.

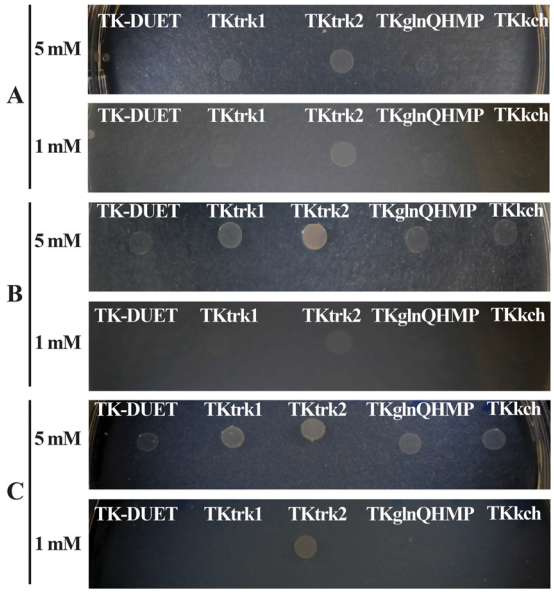

FIG 9 Complementation analysis using *E. coli* TK2420 and its mutant derivatives complemented with *S. mutans* Trk1, Trk2, GlnQHMP, and Kch systems. Strains were grown to mid-exponential phase in HKLM with a high concentration (10 g/liter) of KCl before washing and diluting with K^+-deficient MMGK medium. Cells were spotted on MMGK agar plates with 5 mM KCl (top) or 1 mM KCl (bottom) and selected for ampicillin resistance after incubation for 18 h (A), 36 h (B), and 90 h (C).

port systems is nearly abolished in defined growth medium supplemented with ≤5 mM K^+ (31). We tested if K^+ transport systems from *S. mutans* could restore growth in low K^+ concentrations in growth medium by screening the *E. coli* TK2420 mutant derivatives with Trk1, Trk2, GlnQHMP, or Kch systems that were able to grow on low K^+ (MMGK agar plates containing ≤5 mM K^+). The plates were incubated for up to 90 h to accommodate the cells with slower recovery. Within an 18-h incubation period, we recovered TKtrk2 growth on both 1 mM and 5 mM K^+ plates (Fig. 9). Gradually (36 to 90 h), we also observed recovery of growth of TKtrk1 and TKglnQHMP with 5 mM K^+ supplementation. However, even after 90 h with 1 mM K^+ supplementation, only TKtrk2 grew. Thus, we concluded that Trk2 is an important K^+ transport system that has a crucial function in cell growth under low-K^+ conditions.

The intracellular K^+ concentration was measured for various complemented strains of *E. coli* TK2420 using ICP-OES. Mid-exponential-phase *E. coli* TK2420 and complemented strains were grown in high-K^+ broth (HKLM). Cells were then washed and incubated in MMGK for 2 h before being challenged for K^+ uptake. Trk1, Trk2, and GlnQHMP systems showed a significantly higher acquisition of K^+ (1.234 ± 0.06, 1.488 ± 0.063, and 1.709 ± 0.38 μmol/mg [dry weight] of cells, respectively) than TK2420 cells harboring pET-DUET alone (0.746 ± 0.04 μmol/mg [dry weight] of cells) after 120 s of exposure to 5 mM K^+-supplemented defined MMGK (Fig. 10). TKkch harboring the Kch system showed no difference (0.78 ± 0.05 μmol/mg [dry weight] of cells) compared with TK-DUET, suggesting its inability to acquire K^+ during extracellular availability of 5 mM K^+. These results showed that Trk1, Trk2, and GlnQHMP were able to accumulate significant amounts of K^+ from a low-K^+ extracellular environment (5 mM) within 120 s.

Trk1, Trk2, and GlnQHMP enable *E. coli* TK2420 growth under stress. The role of each of the K^+ transport systems that complemented *E. coli* TK2420 (TKtrk1, TKtrk2, and TKglnQHMP) was assessed in terms of planktonic growth under low-K^+ and high-osmotic-stress (0.4 M NaCl) conditions. The *E. coli* mutant strain TK2420 and its complemented variants harboring Trk1, Trk2, and GlnQHMP systems were initially grown in HKLM and then washed and diluted 1/100 in either LKLM or LKLM with 400 mM NaCl. A control for each strain was prepared similarly, except that the dilution medium contained a high K^+ concentration (HKLM) with 0.4 M NaCl. The growth was monitored in a Bioscreen automated growth-monitoring system for at least 18 h. The complemented strains, TKtrk2 and TKglnQHMP, showed improved growth relative to the deficient strain, TK2420, when grown in low-K^+ medium with or without osmotic stress (see Fig. S2 in the supplemental material), with the most profound improvement being observed in TKtrk2. We also observed that the *pacL* component was able to independently improve the growth of *E. coli* TK2420 up to the levels obtained by TKtrk1 (data not shown). Further, we tested if these systems could accumulate sufficient K^+

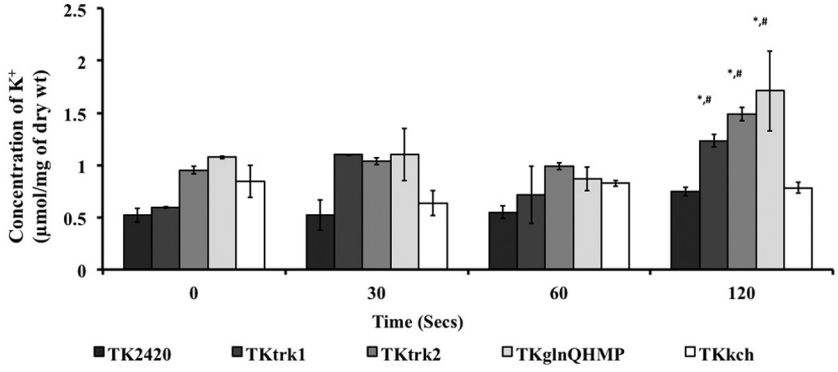

FIG 10 Estimation of intracellular K^+ content in *E. coli* strain TK2420 deficient in major K^+ transport systems and its complemented strains. Strains were grown to mid-exponential phase in K^+-rich KLM medium and incubated in MMGK for 2 h to deplete cellular K^+ levels. Cells were subsequently supplemented with 5 mM KCl and aliquots sampled over time to measure intracellular K^+ content using ICP-OES. Data are representative of two independent experiments performed in duplicate. Error bars represent means ± SD. Repeated-measures ANOVA was used for statistical analysis between different time points compared with the initial time point (*) and between mutants and *E. coli* strain TK2420 harboring an empty vector at the same time point (#).

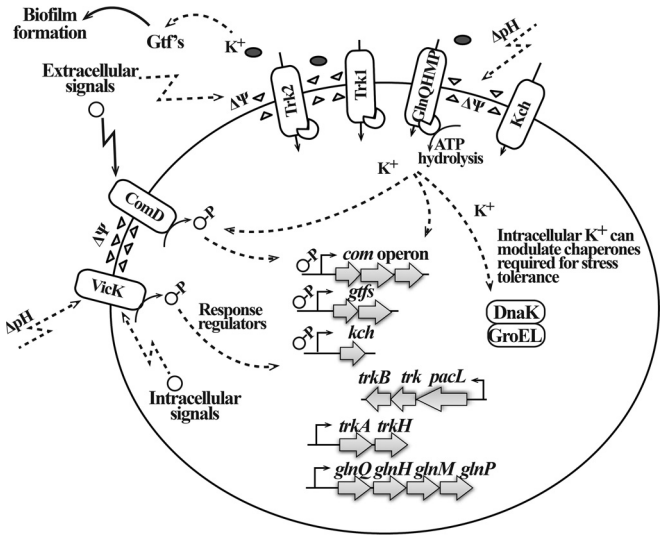

FIG 11 Representation of regulatory mechanisms in *S. mutans* that include K^+ transport systems in physiological responses. Environment changes, including changes in pH and concentration of cations, result in alterations of the membrane physiology, which is sensed by specialized sensing mechanisms. Activation of K^+ accumulation is one way to respond to environmental stress, and high intracellular K^+ concentrations can affect the overall physiological responses of cells by bolstering their defense and repair mechanisms. K^+ levels affect function of important enzymes such as glucosyltransferase, thereby regulating the ability of *S. mutans* to form a biofilm. Although the underlying regulatory mechanism remains to be identified, it is possible that during periods of high K^+ demand, such as under intracellular-K^+-deficient or highly acidic conditions, the membrane proteins (e.g., transport systems) and membrane-bound sensors (e.g., histidine kinases) can respond in a feedback-regulated manner by increasing the inflow of cations (e.g., K^+) through the specific K^+ transport systems.

to aid acid-sensitive *E. coli* TK2420's response to low pH. We observed that both Trk1 (including the individual component PacL) and Trk2 enabled the TK2420 mutant's survival during low-pH (4.0) stress under high-K^+ conditions (see Fig. S2 in the supplemental material). It was concluded from these results that Trk1, Trk2, and GlnQHMP function to accumulate K^+ inside the cells.

Trk proteins influence the membrane potential of *E. coli* TK2420. The alterations in the membrane potential were assayed by measuring the change in fluorescence intensity of $DiSBAC_2(3)$ and normalized with fluorescence intensity decay of dye alone. Our analysis revealed that the TK-DUET strain exhibited a lower intensity change over time in low K^+ (5 mM) in minimal medium or LKLM medium, whereas on addition of 400 mM NaCl, we observed an initial hyperpolarized state (see Fig. S3 in the supplemental material). Upon an increase in extracellular K^+ concentration to ≥25 mM, a more depolarized state was observed. Among TKtrk1, TKtrk2, and TKglnQHMP, we did not observe a profound overall difference, although TKtrk2 had a higher depolarized state than either both TKtrk1 or TKglnQHMP in low K^+ (5 mM) (see Fig. S3 in the supplemental material).

DISCUSSION

S. mutans has highly organized adaptive mechanisms to contend with physiological stress conditions. Here, we have established the mechanism and importance of K^+ uptake and its accumulation in the physiological adaptation to stress. We have determined that K^+ is critical for the growth and survival of *S. mutans*; it acquires K^+ from the extracellular environment via multiple transporters, and K^+ transport systems affect its physiology and virulence attributes. We demonstrated the essentiality of K^+ and the roles of four putative transport systems, Trk1, Trk2, Kch, and GlnQHMP, in K^+ homeostasis of *S. mutans*. Of these, the function of Trk2 was critical to establish a link between extracellular K^+ availability and several virulence attributes of *S. mutans*; for instance, planktonic growth, biofilm formation, and acid tolerance phenotypes were impaired in the absence of Trk2. In the absence of Trk1 and Trk2, *S. mutans* was still capable of acquiring K^+ from its surroundings. While we had previously characterized the function of GlnQHMP in glutamate transport and acid tolerance of *S. mutans* (17), we were able to demonstrate the role of this system in K^+ transport when both Trk1 and Trk2 systems were absent. Loss of the Kch system did not affect K^+ acquisition, growth, or virulence phenotypes in *S. mutans*. Collectively, our results highlight not only the fact that K^+ homeostasis is significant but also the fact that its tight regulation is required to maintain cellular functions.

Previously, effects of K^+ on the growth of *S. mutans* were not investigated in detail. We have shown that *S. mutans* growth is sensitive to extracellular K^+ availability and that low or high K^+ concentrations lead to growth retardation. This result concurs with the previously report showing that high intracellular accumulation of K^+ is required for normal growth and glycolysis in *S. mutans* (15).

K^+ is an important cation in dental plaque fluid, wherein the plaque biofilm constitutes the natural environment of *S. mutans* in the oral cavity. We observed that supplementing cells with K^+ concentrations as low as 5 mM facilitated the formation of robust biofilms, whose biomass remained stable even in K^+ concentrations as high as 150 mM. Effects of K^+ leakage across the membrane and the concentration of extracellular K^+ on biofilm formation in *Bacillus subtilis* have been well studied (42, 43). A possible relationship between K^+ in the biofilm matrix and its integrity was presented in the study by Markevics and Jacques (44), who showed that optimal K^+ in the matrix enhanced the function of glucosyltransferase enzymes of *Streptococcus salivarius*. We demonstrated that the K^+ homeostasis mediated by Trk2 of *S. mutans* affects Gtf function. There are reports suggesting a role for membrane potential in the translocation of proteins across the membrane or their secretion into extracellular spaces (45, 46). It is thus possible that the altered membrane potential due to the K^+ gradient across the membrane in the *trk2*-null mutant could cause the defects in secretion or synthesis of functional Gtf or Gbp proteins that result in an impaired biofilm during sucrose growth under low K^+ conditions. Our Western blots showed that the K^+ perturbation induced by the *trk2* deletion affected the reactivity of cell surface-extracted GtfD to anti-GtfD antibody. We did not, however, observe a significant reduction in the expression levels of the *gtfB* gene in the *trk2*-null mutant compared to its expression in the wild-type strain, suggesting that Gtf secretion may be impaired in the mutant or that some conformational change to the enzyme has occurred during its maturation on the cell surface that alters its detection by the antibody. Morphologically, a dramatic, almost complete absence of glucan puddling around the colonies was observed for the *trk2*-null mutant compared to its wild-type parent strain, UA159, which confirmed that the absence of the Trk2 system affected Gtf activity. The pathway of Gtf secretion is unknown, but it has been suggested that the

Sec pathway is utilized (47). Since fluctuation in the levels of K^+ can affect the oligomeric to monomeric state of SecA cytoplasmic ATPase (48, 49), it seems reasonable that translocation of proteins such as Gtf proteins to the cell surface is affected by K^+ perturbation, as seen in *trk2*-null mutant.

In some bacteria, extracellular K^+ can act as a signal cation to activate virulence mechanisms (50–52). In *S. mutans* Ingbritt, the addition of K^+ increased the rate of acid production, which is an essential virulence factor (14). Another study demonstrated that *S. mutans* K-1 cells grown in K^+-supplemented medium in low pH resulted in increased accumulation of K^+ and increased acid production (53). However, in both of these studies, the authors did not provide the mode of K^+ acquisition and its underlying mechanism. In addition to acid production, tolerance to low pH is an important determinant in maintaining glycolysis and surviving acidic environments, such as those found in carious lesions. A study conducted by Gong et al. examined the acid-induced transcriptome of *S. mutans* and found that the expression of nearly 14% of the genes encoded in its genome was altered by acid stress (54). These included *trkA*, *trkH*, and *trkB*, all of which were significantly upregulated at low pH (54), suggesting their involvement in acid stress tolerance. Our acid tolerance assays confirmed the relationship between the Trk2 system and aciduricity, as the loss of Trk2 resulted in increased susceptibility of cells to acid stress. This mutant was also significantly impaired in its ability to grow and produce acid, whereas SMΔtrk2 showed slower growth than the wild type and SMΔtrk1.

Among various bacterial K^+ transport systems, the Trk systems have gained much attention due to their role in general cell physiology (4) and virulence (31, 55). Here, we noted that *S. mutans* required a 25 mM K^+ concentration in the growth medium to maintain normal cellular activities. The SMΔtrk2 strain and the Trk1/2 double mutants had significantly decreased levels of intracellular K^+ relative to the wild-type strain after 30 min. The diminished ability of these mutants to acquire K^+ likely explains their growth defect (i.e., low final yield) and decreased biofilm biomass compared to the parent strain. The presence of membrane bound and intracellular gating components has been suggested for the TrkAH systems in *Halomonas elongata* (56), *Vibrio alginolyticus* (57), and *Vibrio parahaemolyticus* (58). Proteins similar to Trk proteins have also been shown to function in response to interaction with physiological messengers such as cyclic di-AMP (c-di-AMP) (59, 60). Trk2 in *S. mutans* has two components, which include a membrane-bound TrkH component, which presumably allows the transfer of cations through the cell membrane, and a TrkA component, which likely controls the movement of K^+ into the cytoplasm. In our study, the deletion of either component affected the cellular physiology of *S. mutans* UA159, suggesting that both TrkA and TrkH are required for optimal cellular function. Although we noted an increased ability of the Trk1 mutant to acquire K^+ in the first 2 min, the accrued K^+ levels in this mutant dropped to levels observed in other strains, including the wild type, at later time points. Lack of any other phenotype linked with Trk1 deletion prevented us from concluding the reason underlying the sharp increase observed in K^+ uptake by this mutant. This observation further challenged our initial hypothesis that the *S. mutans* Trk1 acts as a K^+ uptake system, which prompted us to perform complementation studies in an *E. coli* mutant strain unable to transport extracellular K^+.

Each of the K^+ transport systems Trk1, Trk2, GlnQHMP, and Kch was tested for its role in K^+ uptake by complementing the *E. coli* strain TK2420 with these systems. *E. coli* TK2420 is a well-established model organism to characterize K^+ transporters because of its lack of constitutive transporters and inability to transport K^+ (31, 61–63). We observed that complementing *E. coli* TK2420 with Trk1, Trk2, or GlnQHMP facilitated significant K^+ acquisition and enabled normal growth in low K^+ concentrations and under stress conditions imposed by high salt concentrations and low pH. These results confirm the role of Trk1 in K^+ uptake, even though we were unable to functionally dissect these properties in *S. mutans* under our test conditions.

In *S. mutans*, emerging data from microarray studies suggest that K^+ transport systems are linked with the acid stress response (54, 64), sugar transport via the EII component of phospho-transferase system (65), and oxidative stress tolerance (66). Klein and colleagues (67) used *S. mutans* cDNAs derived from biofilms to show that Trk1 component genes, *trkB* and *pacL*, were upregulated when cells were grown in sucrose and starch compared to sucrose alone (67). These authors proposed the role for these genes in osmoregulation of *S. mutans*. Trk proteins in bacteria (other than streptococci) have been shown to function in response to various environmental stressors, such as hypersaline conditions, low pH, oxidative stress, etc. (4, 68). To maintain cellular functions under such stressful conditions, bacteria utilize two forms of metabolic energy obtained by either breakdown of energy-rich phosphate bonds such as ATP or electrochemical energy provided by ion gradients. We postulated that if Trk proteins in *S. mutans* functioned as early stress responders, then they would have a measurable impact on the overall electrochemical membrane potential. In the absence of Trk2, the mutants were unable to grow under hypersaline conditions (Fig. 4) and had altered electropotential gradients in response to extracellular K^+ (see Fig. S1 in the supplemental material). We reasoned that in addition to modulating K^+ import, Trk2 also had a function in contending with osmotic stress. Further, by complementing *E. coli* TK2420 with Trk2, we concluded that the K^+-dependent growth defect under osmotic stress was a direct result of the loss of Trk2 as opposed to simply an indirect physiological response to hyperosmotic stress.

Others have shown a relationship between intracellular Na^+-to-K^+ cationic ratios (69) and pH of the medium, age of the culture, and cell metabolism (70, 71). Since the Na^+-to-K^+ ratios affect the cellular proton motive force (PMF), we investigated how the membrane potential varied under stressful growth conditions (e.g., low pH and osmotic stress). We reasoned that if K^+ acquisition is crucial under these conditions, an efficient K^+ transport system such as Trk2 would be required for cell survival and growth, as shown in our acid tolerance assays. We then hypothesized that in low extracellular K^+, the intracellular levels of K^+ could be manipulated to collapse internal pH homeostasis of cells and affect the transmembrane potential. Cells typically maintain a negative intracellular potential, except for acidophilic cells and except during certain phases in the cell cycle when cells undergo "alternate positive potential" (72). The defect in membrane potential of SMΔtrk2 mutants reinforces its phenotypes' requirement of a high K^+ concentration for cellular functions and pH sensitivity.

In this study, we present an in-depth characterization of four K^+ transport systems in *S. mutans*. In addition to relating K^+ acquisition to growth, we have identified important functions for

this cation and its uptake systems in maintaining virulence properties of *S. mutans*, including acidogenicity, aciduricity, and biofilm formation. Although we outline possible stimuli that may facilitate the exchange or import of K^+ and propose involved pathways based on prior and current knowledge (Fig. 11), the precise mechanisms of their activation and regulatory pathways require further study. Our study highlights the important role of the Trk2 system in *S. mutans* K^+ transport, as well as demonstrating the complexity of other independently functioning, and secondary, multiple K^+ transport systems. This work constitutes the first characterization of the Trk systems in oral streptococci.

ACKNOWLEDGMENTS

Polyclonal anti-Gtf sera were generous gifts from Daniel Smith (Forsyth Dental Institute). We thank Wolfgang Epstein for the *Escherichia coli* TK2420 strain and valuable scientific input throughout the study, Trevor Moraes for kindly providing valuable advice, and Kirsten Krastel and Milos Legner for technical assistance.

This work was supported by CIHR grant MT-15431 to D.G.C.

FUNDING INFORMATION

Gouvernement du Canada | Canadian Institutes of Health Research (CIHR) provided funding to Dennis G. Cvitkovitch under grant number MT-15431.

REFERENCES

1. **Csonka LN.** 1989. Physiological and genetic responses of bacteria to osmotic stress. Microbiol Rev **53:**121–147.
2. **Christian JHB, Waltho JA.** 1961. The sodium and potassium content of non-halophilic bacteria in relation to salt tolerance. J Gen Microbiol **25:** 97–102. http://dx.doi.org/10.1099/00221287-25-1-97.
3. **Booth IR.** 1985. Regulation of cytoplasmic pH in bacteria. Microbiol Rev **49:**359–378.
4. **Epstein W.** 2003. The roles and regulation of potassium in bacteria. Prog Nucleic Acid Res Mol Biol **75:**293–320. http://dx.doi.org/10.1016/S0079-6603(03)75008-9.
5. **Corratgé-Faillie C, Jabnoune M, Zimmermann S, Véry AA, Fizames C, Sentenac H.** 2010. Potassium and sodium transport in non-animal cells: the Trk/Ktr/HKT transporter family. Cell Mol Life Sci **67:**2511–2532. http://dx.doi.org/10.1007/s00018-010-0317-7.
6. **Harold FM, Kakinuma Y.** 1985. Primary and secondary transport of cations in bacteria. Ann N Y Acad Sci **456:**375–383. http://dx.doi.org/10.1111/j.1749-6632.1985.tb14888.x.
7. **Poolman B, Hellingwerf KJ, Konings WN.** 1987. Regulation of the glutamate-glutamine transport system by intracellular pH in Streptococcus lactis. J Bacteriol **169:**2272–2276.
8. **Becker MR, Paster BJ, Leys EJ, Moeschberger ML, Kenyon SG, Galvin JL, Boches SK, Dewhirst FE, Griffen AL.** 2002. Molecular analysis of bacterial species associated with childhood caries. J Clin Microbiol **40:** 1001–1009. http://dx.doi.org/10.1128/JCM.40.3.1001-1009.2002.
9. **Matsui R, Cvitkovitch D.** 2010. Acid tolerance mechanisms utilized by *Streptococcus mutans*. Future Microbiol **5:**403–417. http://dx.doi.org/10.2217/fmb.09.129.
10. **Margolis HC, Moreno EC.** 1994. Composition and cariogenic potential of dental plaque fluid. Crit Rev Oral Biol Med **5:**1–25.
11. **Dibdin GH, Shellis RP, Dawes C.** 1986. A comparison of the potassium content and osmolality of plaque fluid and saliva, and the effects of plaque storage. J Dental Res **65:**1053–1056. http://dx.doi.org/10.1177/00220345860650080301.
12. **Dashper SG, Reynolds EC.** 2000. Effects of organic acid anions on growth, glycolysis, and intracellular pH of oral streptococci. J Dent Res **79:**90–96. http://dx.doi.org/10.1177/00220345000790011601.
13. **Dashper SG, Reynolds EC.** 1992. pH regulation by *Streptococcus mutans*. J Dental Research **71:**1159–1165. http://dx.doi.org/10.1177/00220345920710050601.
14. **Marsh PD, Williamson MI, Keevil CW, McDermid AS, Ellwood DC.** 1982. Influence of sodium and potassium ions on acid production by washed cells of *Streptococcus mutans* Ingbritt and *Streptococcus sanguis* NCTC 7865 grown in a chemostat. Infect Immun **36:**476–483.
15. **Dashper SG, Reynolds EC.** 1996. Lactic acid excretion by *Streptococcus mutans*. Microbiology **142:**33–39. http://dx.doi.org/10.1099/13500872-142-1-33.
16. **Sato Y, Noji S, Suzuki R, Taniguchi S.** 1989. Dual mechanism for stimulation of glutamate transport by potassium ions in *Streptococcus mutans*. J Bacteriol **171:**4963–4966.
17. **Krastel K, Senadheera DB, Mair R, Downey JS, Goodman SD, Cvitkovitch DG.** 2010. Characterization of a glutamate transporter operon, *glnQHMP*, in *Streptococcus mutans* and its role in acid tolerance. J Bacteriol **192:**984–993. http://dx.doi.org/10.1128/JB.01169-09.
18. **Fujiwara S, Kobayashi S, Nakayama H.** 1978. Development of a minimal medium for *Streptococcus mutans*. Arch Oral Biol **23:**601–602. http://dx.doi.org/10.1016/0003-9969(78)90280-7.
19. **Parfenova LV, Rothberg BS.** 2006. Genetic screening for functionality of bacterial potassium channel mutants using K+ uptake-deficient *Escherichia coli*. Methods Mol Biol **337:**157–165.
20. **Lau PCY, Sung CK, Lee JH, Morrison DA, Cvitkovitch DG.** 2002. PCR ligation mutagenesis in transformable streptococci: application and efficiency. J Microbiol Methods **49:**193–205. http://dx.doi.org/10.1016/S0167-7012(01)00369-4.
21. **Li Y-H, Lau PCY, Tang N, Svensäter G, Ellen RP, Cvitkovitch DG.** 2002. Novel two-component regulatory system involved in biofilm formation and acid resistance in *Streptococcus mutans*. J Bacteriol **184:**6333–6342. http://dx.doi.org/10.1128/JB.184.22.6333-6342.2002.
22. **Li Y-H, Hanna MN, Svensäter G, Ellen RP, Cvitkovitch DG.** 2001. Cell density modulates acid adaptation in *Streptococcus mutans*: implications for survival in biofilms. J Bacteriol **183:**6875–6884. http://dx.doi.org/10.1128/JB.183.23.6875-6884.2001.
23. **Li Y-H, Lau PCY, Lee JH, Ellen RP, Cvitkovitch DG.** 2001. Natural genetic transformation of *Streptococcus mutans* growing in biofilms. J Bacteriol **183:**897–908. http://dx.doi.org/10.1128/JB.183.3.897-908.2001.
24. **Xiao J, Klein MI, Falsetta ML, Lu B, Delahunty CM, Yates JR III, Heydorn A, Koo H.** 2012. The exopolysaccharide matrix modulates the interaction between 3D architecture and virulence of a mixed-species oral biofilm. PLoS Pathog **8:**e1002623. http://dx.doi.org/10.1371/journal.ppat.1002623.
25. **Koo H, Xiao J, Klein MI, Jeon JG.** 2010. Exopolysaccharides produced by *Streptococcus mutans* glucosyltransferases modulate the establishment of microcolonies within multispecies biofilms. J Bacteriol **192:**3024–3032. http://dx.doi.org/10.1128/JB.01649-09.
26. **Ajdić D, Pham VTT.** 2007. Global transcriptional analysis of *Streptococcus mutans* sugar transporters using microarrays. J Bacteriol **189:**5049–5059. http://dx.doi.org/10.1128/JB.00338-07.
27. **Hanna MN, Ferguson RJ, Li Y-H, Cvitkovitch DG.** 2001. *uvrA* is an acid-inducible gene involved in the adaptive response to low pH in *Streptococcus mutans*. J Bacteriol **183:**5964–5973. http://dx.doi.org/10.1128/JB.183.20.5964-5973.2001.
28. **Pfaffl MW.** 2001. A new mathematical model for relative quantification in real-time RT–PCR. Nucleic Acids Res **29:**e45–e45. http://dx.doi.org/10.1093/nar/29.9.e45.
29. **Smith DJ, Akita H, King WF, Taubman MA.** 1994. Purification and antigenicity of a novel glucan-binding protein of *Streptococcus mutans*. Infect Immun **62:**2545–2552.
30. **Sorio C, Buffelli M, Angiari C, Ettorre M, Johansson J, Vezzalini M, Viviani L, Ricciardi M, Verzè G, Assael BM, Melotti P.** 2011. Defective CFTR expression and function are detectable in blood monocytes: development of a new blood test for cystic fibrosis. PLoS One **6:**e22212. http://dx.doi.org/10.1371/journal.pone.0022212.
31. **Buurman ET, McLaggan D, Naprstek J, Epstein W.** 2004. Multiple paths for nonphysiological transport of K+ in *Escherichia coli*. J Bacteriol **186:** 4238–4245. http://dx.doi.org/10.1128/JB.186.13.4238-4245.2004.
32. **Marchler-Bauer A, Derbyshire MK, Gonzales NR, Lu S, Chitsaz F, Geer LY, Geer RC, He J, Gwadz M, Hurwitz DI, Lanczycki CJ, Lu F, Marchler GH, Song JS, Thanki N, Wang Z, Yamashita RA, Zhang D, Zheng C, Bryant SH.** 2015. CDD: NCBI's conserved domain database. Nucleic Acids Res **43:**D222–226. http://dx.doi.org/10.1093/nar/gku1221.
33. **Sansom MS, Shrivastava IH, Bright JN, Tate J, Capener CE, Biggin PC.** 2002. Potassium channels: structures, models, simulations. Biochim Biophys Acta **1565:**294–307. http://dx.doi.org/10.1016/S0005-2736(02)00576-X.
34. **Svensater G, Larsson UB, Greif EC, Cvitkovitch DG, Hamilton IR.**

1997. Acid tolerance response and survival by oral bacteria. Oral Microbiol Immunol **12:**266–273. http://dx.doi.org/10.1111/j.1399-302X.1997.tb00390.x.

35. **Svensater G, Sjogreen B, Hamilton IR.** 2000. Multiple stress responses in *Streptococcus mutans* and the induction of general and stress-specific proteins. Microbiology **146:**107–117. http://dx.doi.org/10.1099/00221287-146-1-107.
36. **Abranches J, Lemos JA, Burne RA.** 2006. Osmotic stress responses of *Streptococcus mutans* UA159. FEMS Microbiol Lett **255:**240–246. http://dx.doi.org/10.1111/j.1574-6968.2005.00076.x.
37. **Nishimura J, Saito T, Yoneyama H, Lan Bai L, Okumura K, Isogai E.** 2012. Biofilm formation by *Streptococcus mutans* and related bacteria. Adv Microbiol **2:**208–215. http://dx.doi.org/10.4236/aim.2012.23025.
38. **Marsh PD.** 2004. Dental plaque as a microbial biofilm. Caries Res **38:**204–211. http://dx.doi.org/10.1159/000077756.
39. **Klein MI, Duarte S, Xiao J, Mitra S, Foster TH, Koo H.** 2009. Structural and molecular basis of the role of starch and sucrose in *Streptococcus mutans* biofilm development. Appl Environ Microbiol **75:**837–841. http://dx.doi.org/10.1128/AEM.01299-08.
40. **Strahl H, Hamoen LW.** 2010. Membrane potential is important for bacterial cell division. Proc Natl Acad Sci U S A **107:**12281–12286. http://dx.doi.org/10.1073/pnas.1005485107.
41. **Gášková D, Brodská B, Heřman P, Večeř J, Malínský J, Sigler K, Benada O, Plášek J.** 1998. Fluorescent probing of membrane potential in walled cells: diS-C3(3) assay in *Saccharomyces cerevisiae*. Yeast **14:**1189–1197.
42. **López D, Gontang EA, Kolter R.** 2010. Potassium sensing histidine kinase in *Bacillus subtilis*. Methods Enzymol **471:**229–251. http://dx.doi.org/10.1016/S0076-6879(10)71013-2.
43. **Fall R, Kearns DB, Nguyen T.** 2006. A defined medium to investigate sliding motility in a *Bacillus subtilis* flagella-less mutant. BMC Microbiol **6:**31. http://dx.doi.org/10.1186/1471-2180-6-31.
44. **Markevics LJ, Jacques NA.** 1985. Enhanced secretion of glucosyltransferase by changes in potassium ion concentrations is accompanied by an altered pattern of membrane fatty acids in *Streptococcus salivarius*. J Bacteriol **161:**989–994.
45. **Daniels CJ, Bole DG, Quay SC, Oxender DL.** 1981. Role for membrane potential in the secretion of protein into the periplasm of *Escherichia coli*. Proc Natl Acad Sci U S A **78:**5396–5400. http://dx.doi.org/10.1073/pnas.78.9.5396.
46. **Palmen R, Driessen AJ, Hellingwerf KJ.** 1994. Bioenergetic aspects of the translocation of macromolecules across bacterial membranes. Biochim Biophys Acta **1183:**417–451. http://dx.doi.org/10.1016/0005-2728(94)90072-8.
47. **Huang M, Meng L, Fan M, Hu P, Bian Z.** 2008. Effect of biofilm formation on virulence factor secretion via the general secretory pathway in *Streptococcus mutans*. Arch Oral Biol **53:**1179–1185. http://dx.doi.org/10.1016/j.archoralbio.2008.07.007.
48. **Economou A, Pogliano JA, Beckwith J, Oliver DB, Wickner W.** 1995. SecA membrane cycling at SecYEG is driven by distinct ATP binding and hydrolysis events and is regulated by SecD and SecF. Cell **83:**1171–1181. http://dx.doi.org/10.1016/0092-8674(95)90143-4.
49. **Wowor AJ, Yu D, Kendall DA, Cole JL.** 2011. Energetics of SecA Dimerization. J Mol Biol **408:**87–98. http://dx.doi.org/10.1016/j.jmb.2011.02.006.
50. **Xue T, You Y, Hong D, Sun H, Sun B.** 2011. The *Staphylococcus aureus* KdpDE two-component system couples extracellular K+ sensing and Agr signaling to infection programming. Infect Immun **79:**2154–2167. http://dx.doi.org/10.1128/IAI.01180-10.
51. **Su J, Gong H, Lai J, Main A, Lu S.** 2009. The potassium transporter Trk and external potassium modulate *Salmonella enterica* protein secretion and virulence. Infect Immun **77:**667–675. http://dx.doi.org/10.1128/IAI.01027-08.
52. **Gries CM, Bose JL, Nuxoll AS, Fey PD, Bayles KW.** 2013. The Ktr potassium transport system in *Staphylococcus aureus* and its role in cell physiology, antimicrobial resistance and pathogenesis. Mol Microbiol **89:**760–773. http://dx.doi.org/10.1111/mmi.12312.
53. **Luoma H.** 1971. Potassium and sodium content and acid production of nongrowing cariogenic streptococci. Eur J Oral Sciences **79:**202–208. http://dx.doi.org/10.1111/j.1600-0722.1971.tb02010.x.
54. **Gong Y, Tian X-L, Sutherland T, Sisson G, Mai J, Ling J, Li Y-H.** 2009. Global transcriptional analysis of acid-inducible genes in *Streptococcus mutans*: multiple two-component systems involved in acid adaptation. Microbiology **155:**3322–3332. http://dx.doi.org/10.1099/mic.0.031591-0.
55. **Alkhuder K, Meibom KL, Dubail I, Dupuis M, Charbit A.** 2010. Identification of *trkH*, encoding a potassium uptake protein required for *Francisella tularensis* systemic dissemination in mice. PLoS One **5:**e8966. http://dx.doi.org/10.1371/journal.pone.0008966.
56. **Kraegeloh A, Amendt B, Kunte HJ.** 2005. Potassium transport in a halophilic member of the Bacteria domain: identification and characterization of the K+ uptake systems TrkH and TrkI from *Halomonas elongata* DSM 2581T. J Bacteriol **187:**1036–1043. http://dx.doi.org/10.1128/JB.187.3.1036-1043.2005.
57. **Nakamura T, Yamamuro N, Stumpe S, Unemoto T, Bakker EP.** 1998. Cloning of the *trkAH* gene cluster and characterization of the Trk K+-uptake system of *Vibrio alginolyticus*. Microbiology **144:**2281–2289. http://dx.doi.org/10.1099/00221287-144-8-2281.
58. **Cao Y, Pan Y, Huang H, Jin X, Levin EJ, Kloss B, Zhou M.** 2013. Gating of the TrkH ion channel by its associated RCK protein TrkA. Nature **496:**317–322. http://dx.doi.org/10.1038/nature12056.
59. **Corrigan RM, Campeotto I, Jeganathan T, Roelofs KG, Lee VT, Gründling A.** 2013. Systematic identification of conserved bacterial c-di-AMP receptor proteins. Proc Natl Acad Sci U S A **110:**9084–9089. http://dx.doi.org/10.1073/pnas.1300595110.
60. **Bai Y, Yang J, Zarrella TM, Zhang Y, Metzger DW, Bai G.** 2014. Cyclic di-AMP impairs potassium uptake mediated by a cyclic di-aMP binding protein in *Streptococcus pneumoniae*. J Bacteriol **196:**614–623. http://dx.doi.org/10.1128/JB.01041-13.
61. **Sturr MG, Ablooglu AJ, Krulwich TA.** 1997. A *Bacillus subtilis* locus encoding several gene products affecting transport of cations. Gene **188:**91–94. http://dx.doi.org/10.1016/S0378-1119(96)00784-6.
62. **Kitko RD, Wilks JC, Garduque GM, Slonczewski JL.** 2010. Osmolytes contribute to pH homeostasis of *Escherichia coli*. PLoS One **5:**e10078. http://dx.doi.org/10.1371/journal.pone.0010078.
63. **Sun S, Gan JH, Paynter JJ, Tucker SJ.** 2006. Cloning and functional characterization of a superfamily of microbial inwardly rectifying potassium channels. Physiol Genomics **26:**1–7. http://dx.doi.org/10.1152/physiolgenomics.00026.2006.
64. **Senadheera D, Krastel K, Mair R, Persadmehr A, Abranches J, Burne RA, Cvitkovitch DG.** 2009. Inactivation of VicK affects acid production and acid survival of *Streptococcus mutans*. J Bacteriol **191:**6415–6424. http://dx.doi.org/10.1128/JB.00793-09.
65. **Abranches J, Candella MM, Wen ZT, Baker HV, Burne RA.** 2006. Different roles of EIIABMan and EIIGlc in regulation of energy metabolism, biofilm development, and competence in *Streptococcus mutans*. J Bacteriol **188:**3748–3756. http://dx.doi.org/10.1128/JB.00169-06.
66. **Ahn S-J, Wen ZT, Burne RA.** 2007. Effects of oxygen on virulence traits of *Streptococcus mutans*. J Bacteriol **189:**8519–8527. http://dx.doi.org/10.1128/JB.01180-07.
67. **Klein MI, DeBaz L, Agidi S, Lee H, Xie G, Lin AHM, Hamaker BR, Lemos JA, Koo H.** 2010. Dynamics of *Streptococcus mutans* transcriptome in response to starch and sucrose during biofilm development. PLoS One **5:**e13478. http://dx.doi.org/10.1371/journal.pone.0013478.
68. **Holtmann G, Bakker EP, Uozumi N, Bremer E.** 2003. KtrAB and KtrCD: two K+ uptake systems in *Bacillus subtilis* and their role in adaptation to hypertonicity. J Bacteriol **185:**1289–1298. http://dx.doi.org/10.1128/JB.185.4.1289-1298.2003.
69. **Schultz SG, Solomon AK.** 1961. Cation transport in *Escherichia coli*. I. Intracellular Na and K concentrations and net cation movement. J Gen Physiol **45:**355–369.
70. **Epstein W, Kim BS.** 1971. Potassium transport loci in *Escherichia coli* K-12. J Bacteriol **108:**639–644.
71. **Ignatov OV, Gribanova YS, Shchegolev SY, Bunin VD, Ignatov VV.** 2002. The electro-optical investigation of suspensions of *Escherichia coli* K-12 cells metabolizing glucose, lactose, and galactose. Microbiology **71:**302–305. http://dx.doi.org/10.1023/A:1015854611552.
72. **Ivanov V, Rezaeinejad S, Chu J.** 2013. Cell dualism: presence of cells with alternative membrane potentials in growing populations of bacteria and yeasts. J Bioenerg Biomembr **45:**505–510. http://dx.doi.org/10.1007/s10863-013-9515-y.